SAE International

2012-01-1551
Published
06/13/2012

Modeling Interior Noise due to Fluctuating Surface Pressures from Exterior flows

Phil Shorter, Denis Blanchet and Vincent Cotoni
ESI

doi:10.4271/2012-01-1551

ABSTRACT

There are many applications in which exterior flow over a structure is an important source for interior noise. In order to predict interior "wind noise" it is necessary to model both: (i) the spatial and spectral statistics of the exterior fluctuating surface pressures (across a broad frequency range) and (ii) the way in which these fluctuating surface pressures are transmitted through a structure and radiated as interior noise (across a broad frequency range). One approach to the former is to use an unsteady CFD model. While CFD is used routinely for external aerodynamics, its application to the characterization of exterior fluctuating surface pressures for broadband interior noise problems is relatively new. Accurate prediction of both the convective and acoustic wavenumber content of the flow across a broad frequency range can therefore present some challenges. This paper presents a numerical investigation of the spatial and spectral statistics contained in the flow downstream of a simplified side-mirror. Two distinct concentrations of energy are observed in wavenumber space at the convective and acoustic wavenumbers. This therefore opens up the possibility of describing a complex windnoise source in terms of the superposition of two simple analytical sources that can be fit to CFD data.

INTRODUCTION

The term 'windnoise' is often used to describe interior noise that is generated by unsteady exterior flows. In transportation applications, excessive windnoise affects interior comfort and can result in negative perceptions of vehicle quality [1]. There is therefore significant interest in being able to predict windnoise upfront in the design process in order to reduce source content and modify paths (to meet cost, weight and noise targets). In order to model windnoise it is necessary to understand the source (the fluctuating surface pressures on certain exterior regions of a structure), the paths (which typically involve direct vibro-acoustic transmission through certain regions of the structure, transmission through nearby leaks/seals and isolation and absorption provided by the interior sound package) and the receiver (in particular, the frequency range(s) in which windnoise provides an audible contribution to the interior noise in the occupant headspaces). While many regions of a vehicle can contribute to windnoise, the fluctuating surface pressures on the front sideglass (due to vortices and separated flow generated by the A-pillar and mirror) are often an important contributor. This paper therefore considers an analysis of the fluctuating surface pressures downstream of a simplified side mirror as shown in Figure 1. The mirror is mounted in the floor of a windtunnel and was used in a recent JSAE benchmark study that compared (exterior) aero-acoustic predictions from various commercial CFD codes [2] (additional details about the flow conditions and geometry can be found in the reference). While the prediction of far-field exterior aero-acoustic noise is useful for benchmarking the far-field aero-acoustic analogies in different CFD codes, it is often found that changes in far-field exterior noise do not correlate with changes in interior noise (far-field exterior noise measurements are therefore not sufficient to characterize interior wind noise). One reason for this is that the structure acts as a spatial filter and preferentially transmits certain wavenumbers in the fluctuating surface pressure [3].

The spatial filtering of different exterior fluctuating surface pressures can be demonstrated using a simple numerical example. Figure 2 shows two glass panels of dimension 1 × 1 × 4e-3m. Each has a constant damping loss factor of 6% and is placed in contact with a 1 m^3 acoustic cavity. A Diffuse Acoustic Field excitation is applied to the first panel and a Turbulent Boundary Layer (with a 50 m/s free stream

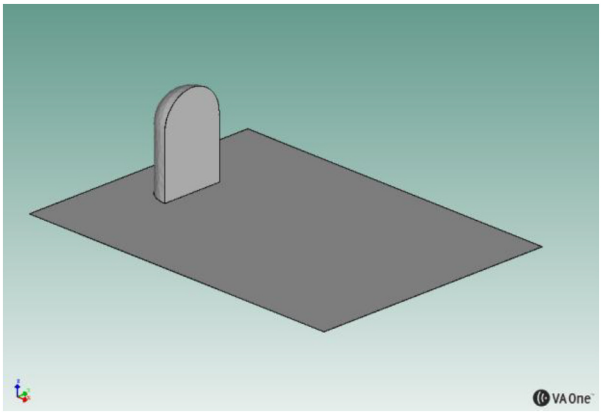

Figure 1. Simplified side-mirror located in the floor of an (anechoic) windtunnel.

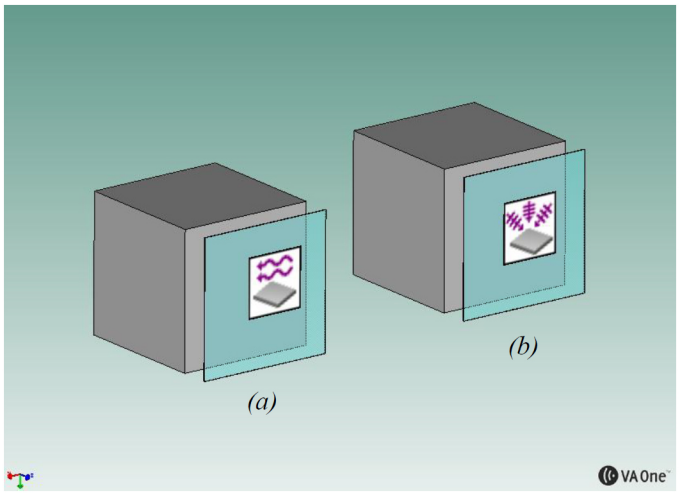

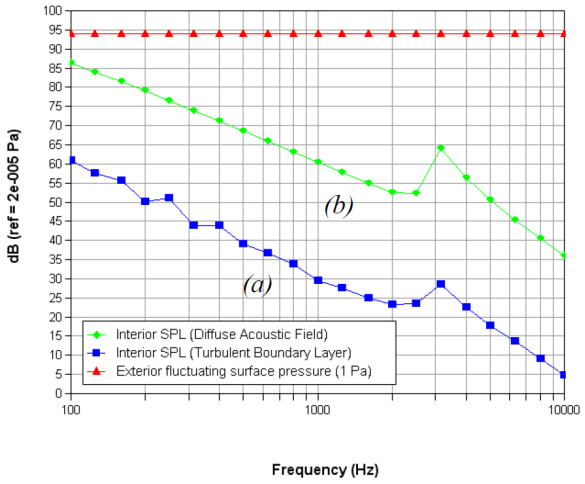

Figure 2. Glass panel of dimension 1×1×4e-3m in contact with a 1m^3 acoustic cavity and excited by (a) Turbulent Boundary Layer (with a 50 m/s mean flow) and (b) Diffuse Acoustic Field. Prediction of interior SPL when each exterior load is normalized to have a unit exterior fluctuating surface pressure. Note the large differences in interior SPL due to the different spatial correlation characteristics of each load.

velocity) is applied to the second panel. The magnitude of the exterior fluctuating surface pressure of each load has been normalized to have unit amplitude. An SEA model is then used to predict the interior sound pressure levels of each cavity [4]. It can be seen in Figure 2 that even though both loads have the same exterior fluctuating surface pressure level, the interior sound pressure level due to the Turbulent Boundary Layer is approximately 30dB lower than that due to the diffuse acoustic field (it is noted in passing that the peak in the interior SPL around 3kHz is associated with the glass coincidence frequency).

The reason for the difference in interior SPL is due to differences in the "spatial correlation" of the two loads. The cross-spectra S_{pp} between two locations in a spatially homogenous fluctuating surface pressure can be written as

$$Spp(x,x') = F(\omega)R(x,x',\omega) \tag{1}$$

Where F is a function of frequency (that does not depend on location) and R represents a spatial correlation function. A diffuse acoustic field has a spatial correlation function R of the form [5]

$$R(x,x') = \sin(kr)/kr; \quad r = |x - x'| \tag{2}$$

where k is the acoustic wavenumber and r is the distance between two locations x and x' on the surface. A Turbulent Boundary Layer (modeled using a Corcos type model) has a spatial correlation function R of the form [6]

$$R(\Delta x,\Delta y) = \exp\left(-\alpha_x|\Delta x| - \alpha_y|\Delta y|\right)\exp\left(-ik_c\Delta x\right) \tag{3}$$

where Δx is the separation between two points in the flow direction, Δy is the separation in the cross flow direction, α_x and α_y are decay coefficients in the flow and cross-flow directions and k_c is the convection wavenumber.

For the sideglass problem, the acoustic wavenumber is typically much lower than the convection wavenumber across much of the frequency range of interest (the diffuse acoustic field has a much longer spatial correlation length than the Turbulent Boundary Layer). The two different excitations therefore result in very different distributions of energy in wavenumber space, and this preferentially excites different structural mode shapes of the glass. The diffuse acoustic field has a concentration of energy at low wavenumbers (wavenumbers that are contained within the 'acoustic circle'). Below coincidence, this typically excites the 'non-resonant' (mass controlled) modes of the glass. Since these modes are also efficient acoustic radiators, the mass controlled modes are typically the dominant transmission path below coincidence. Above coincidence, the resonant modes become the dominant transmission path but these modes are also well excited by the wavenumber content of a diffuse acoustic field. In contrast, a Turbulent Boundary Layer typically has a concentration of energy at the convective wavenumber of the flow and has much smaller concentrations of energy at the wavenumbers associated with the resonant and mass controlled modes of the panel. The net result is that a diffuse acoustic field is transmitted through the glass much more efficiently than a Turbulent Boundary Layer with the same RMS fluctuating surface pressure.

In summary, in order to characterize an exterior fluctuating surface pressure it is necessary to be able to characterize not only the magnitude of the fluctuating surface pressure but also the wavenumber content. A number of different models have been proposed previously for describing the wavenumber content of the fluctuating surface pressures on a sideglass. One approach is to measure overall fluctuating surface pressures, assume these are dominated by the convective component and then use a semi-empirical method to relate the relative amplitudes of the acoustic and convective components of the flow (this is done implicitly in the work discussed in [7,8,9,10] through the definition of an area coupling between two cavities with different wave speeds). While this approach is applicable to certain geometries, there is no guarantee that the empirical relation between the amplitudes of the two components is generally applicable. An alternative approach is therefore to use a CFD model to predict the fluctuating surface pressures and to try to use various signal processing techniques to characterize the wavenumber content of the fluctuating surface pressures. This is discussed in more detail in the following sections.

FLOW PAST SIMPLIFIED SIDE MIRROR

An unsteady CFD analysis was performed for flow past the simplified side mirror described in [2]. Figure 3 shows examples of the unsteady flow due to a free-stream velocity of 50m/s (computed using the commercial code in [11]). Additional details about the CFD model and boundary conditions can be found in [2]. The fluctuating wall pressures were recovered for a rectangular region of dimension 0.45m × 0.2m downstream of the side mirror as shown in Figure 4. A time segment of length 0.05 seconds was recorded using an average time step size of approximately 1e-5 seconds. The overall level of the surface pressure is shown in Figure 4. The pressure time history data was then imported into the commercial vibro-acoustics software in [4]. The time domain data was converted to the frequency domain and averaged over 8 segments with 50% overlap (the resulting cross-spectral data was then integrated onto a $1/12^{th}$ octave frequency domain). The magnitude of the auto-spectra in the 100Hz and 1kHz $1/12^{th}$ octave bands are plotted in Figure 5. The shorter spatial structures in the flow at higher frequencies are clearly visible.

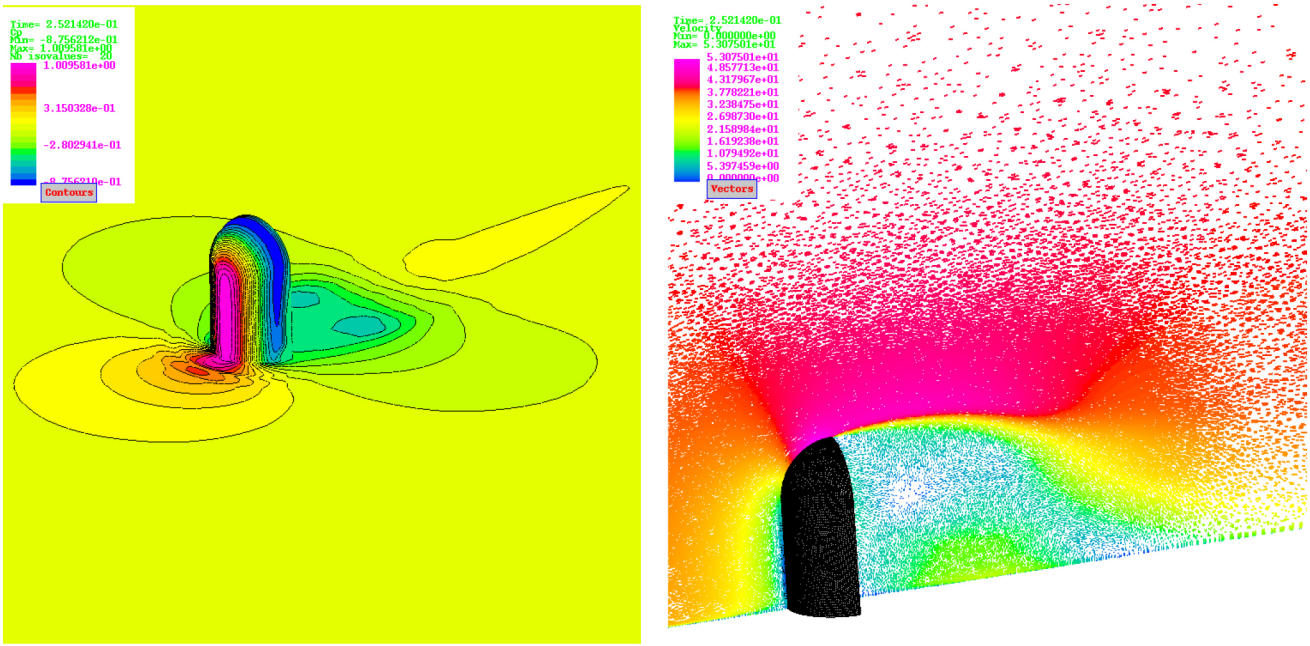

Figure 3. Visualization of flow predicted by CFD code: (a) Cp distribution and (b) velocity vectors.

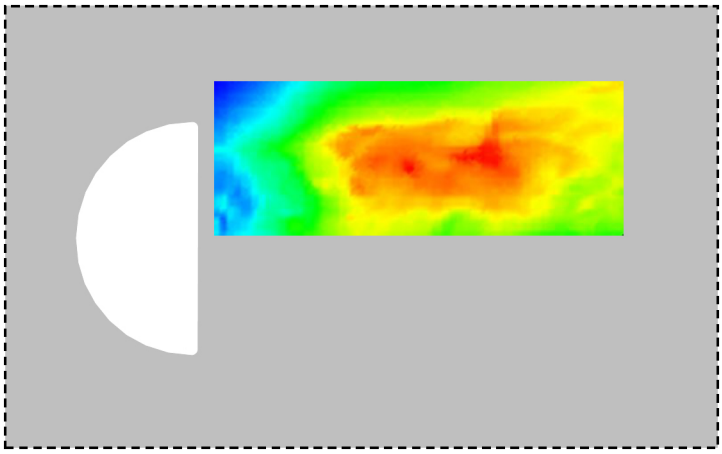

Figure 4. Geometric region downstream of side mirror of dimension 0.45m × 0.2m used for analysis of Fluctuating Surface Pressures. Overall level of fluctuating surface pressure plotted (using a 30dB scale).

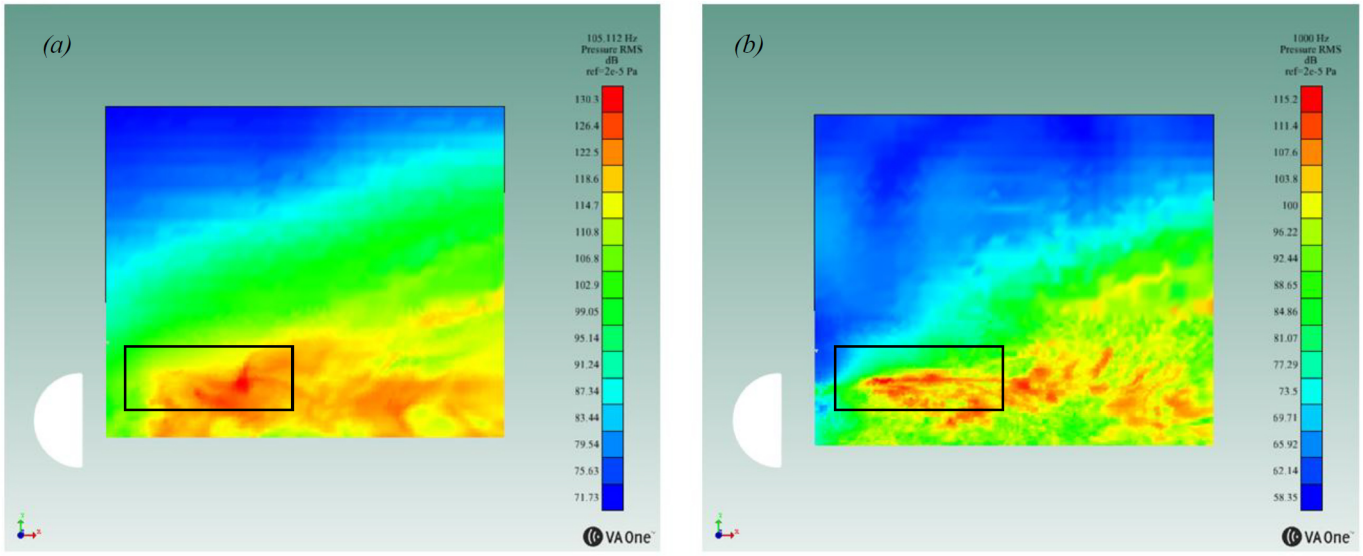

Figure 5. Magnitude of Fluctuating Surface pressure at: (a) 100 Hz and (b) 1kHz. Region of interest shown with black rectangle. Note the shorter spatial structures in the flow at higher frequencies

SPATIAL CORRELATION

Visualization of the auto-spectra of the flow is useful for understanding the flow characteristics, however, as discussed in the opening section it does not provide any information about the spatial correlation (or wavenumber content) of the fluctuating surface pressures. Additional signal processing was therefore performed using the Aero-Vibro-Acoustics module in [4]. In particular, the full cross-spectral matrix was calculated for a (dense) grid of points across the surface region of interest. This surface region was divided into a (coarser) orthogonal grid and a reduced cross-spectral matrix obtained by averaging the auto-spectra and cross-spectra within each cell of the coarse grid. Spatial correlation functions R were then obtained by averaging overall all pairs of cells with the same separation distance in the flow and cross-flow directions. The resulting space averaged correlation function in the flow direction is shown by the red curves in Figure 6 (at 300Hz and 3.25kHz). For comparison, the analytical expression for the spatial correlation in a diffuse field is also shown by the blue curves (with an acoustic wavenumber k = 5.3 rad/m). It can be seen that at low frequencies (Figure 6a), the spatial correlation in the CFD results decays much more rapidly than would occur in a diffuse acoustic field. The parameters of a Corcos TBL can be fitted to the CFD results using the algorithms implemented in [4]. It can be seen that a Corcos TBL model with a convection wavenumber k_c = 62 rad/m provides a good fit to the spatial correlation in the CFD data. This convection wavenumber is physically plausible and represents a convection velocity that is approximately 60% of the free

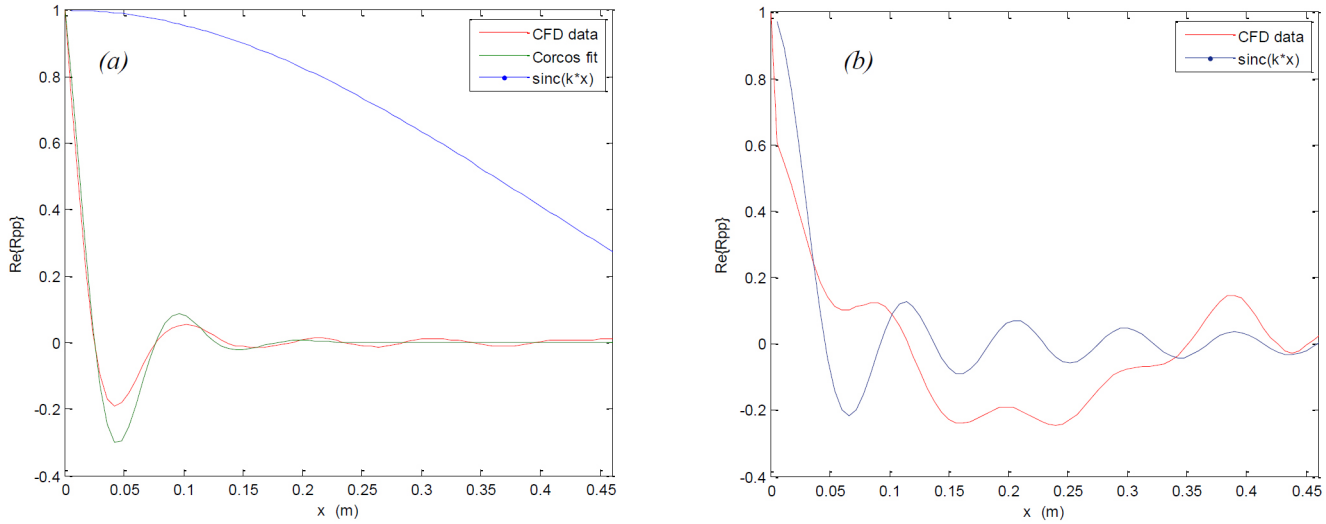

Figure 6. Spatial correlation in flow-direction at: (a) 300Hz and (b) 3250 Hz. Solid black line, post-processed CFD data; dashed line, expected spatial correlation in a diffuse acoustic field; gray line, expected spatial correlation in a Corcos turbulent boundary layer fit to CFD convection velocity.

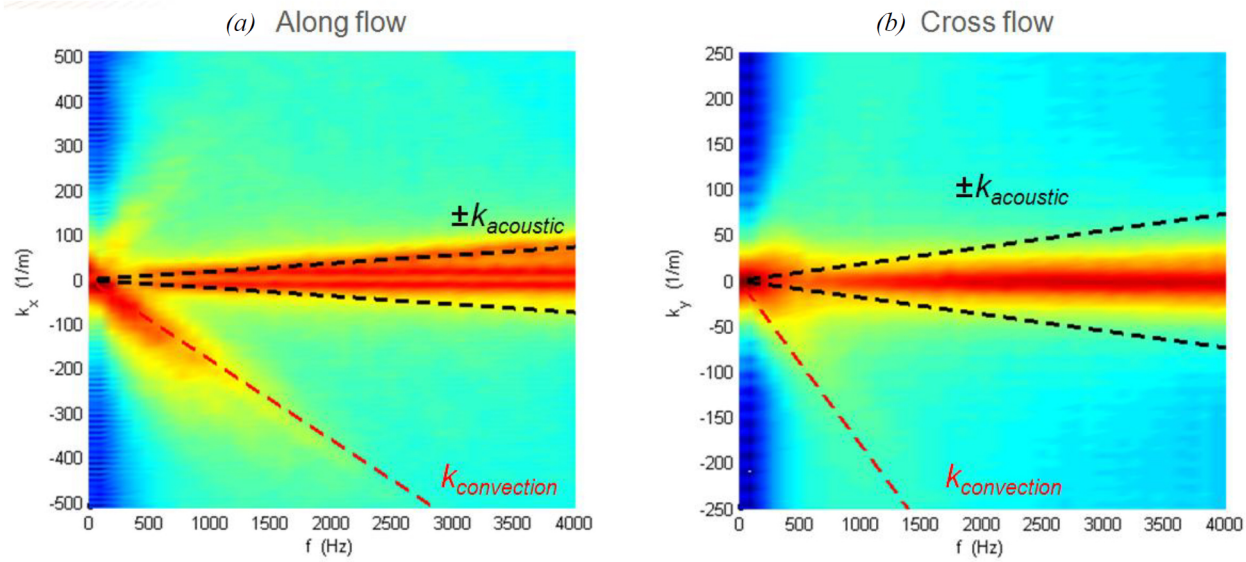

Figure 7. Wavenumber content of spatial correlation in flow and cross-flow directions.

stream velocity. At higher frequencies, (Figure 6b), the oscillations in the spatial correlation match those of a propagating acoustic wave. The decay in the spatial correlation does not exactly match that of a spatially homogenous diffuse-acoustic field. However, this is perhaps to be expected since the fluctuating surface pressure is not homogenous and is therefore likely to exhibit non-uniform acoustic directivity.

WAVENUMBER CONTENT

The wavenumber content in the flow and cross-flow directions can be obtained by calculating the wavenumber transform of the spatial correlation functions obtained in the previous section (at each frequency of interest). The magnitude of the wavenumber transforms are plotted in Figure 7 (the scale of the contour plot is approximately 30dB). The wavenumber of a freely propagating acoustic wave (in the upstream and downstream directions) is also plotted as a dashed black line in the Figure. It can be seen that there is a distinct concentration of energy associated with acoustic wave propagation across the frequency range of interest. In the flow direction, this energy is spread across several different angles of incidence (and hence occurs at all wavenumbers < $k_{acoustic}$). A slight Doppler shift can also be seen in the acoustic wavenumbers in the flow direction. Acoustic waves travelling upstream have a slower overall wavespeed and hence higher wavenumbers than acoustic

waves that travel downstream. From Figure 7b, it can be seen that there are relatively few acoustic waves that propagate directly in the cross-flow direction. Instead, the waves tend to travel at an angle to the cross-flow direction (and hence have a smaller wavenumber in the cross-flow direction). This suggests a directional acoustic source (possibly associated with the fluctuating surface pressures on the mirror acting as an acoustic source).

The convection wavenumber for a typical TBL has also been plotted as a dashed red line in the Figure. It can be seen that at low frequencies (below 1kHz) there is a distinct concentration of energy at the convective wavenumber in the flow direction. However, at higher frequencies there is little evidence of any energy at the convective wavenumber. This may be physical but it may also perhaps be an artifact of the CFD calculation (and due to difficulties resolving the short spatial correlation lengths at higher frequencies with a given mesh size). As expected, there is little evidence of any convection in the cross-flow direction.

Comparing Figure 5 and Figure 7, it can be seen that a complex distribution of energy in the spatial domain becomes a much simpler distribution of energy in the wavenumber domain. While not discussed explicitly in this paper, it is possible to fit simple TBL and acoustic loads to the energy in wavenumber space. The accuracy of this approach is currently the subject of ongoing work and will be reported in separate publications.

SUMMARY/CONCLUSIONS

This paper has provided a numerical investigation of the spatial and spectral statistics of the fluctuating wall pressures downstream of a simplified side-mirror. The importance of spatial correlation when characterizing fluctuating surface pressures was emphasized using a simple example. The transmission of sound through a glass panel was compared when excited by a turbulent boundary layer and a diffuse acoustic field. For the same exterior pressure level, the turbulent boundary layer resulted in interior sound pressure levels that were 30dB less than for the diffuse acoustic field. The fluctuating pressure levels downstream of a simplified side-mirror were then investigated. By performing a number of signal processing operations it was possible to plot the wavenumber content of the spatial correlation (averaged across a region of interest). Clear concentrations of energy were seen at the convective and acoustic wavenumbers. This therefore opens up the possibility of fitting analytical turbulent boundary layer and diffuse acoustic field loads to post-processed CFD results in order to provide simple windnoise sources in vibro-acoustic models.

REFERENCES

1. Power, J.D. 2011 Initial Quality Survey : http:// www.jdpower.com/

2. Itoh, Y. et al. "A CFD Benchmark for Aero-Acoustic Noise Radiated from Simplified Door-Mirror Model". Proc. Japanese Society of Automotive Engineers (JSAE), May 2010.

3. Bremner, P., Wilby, J. "AERO-VIBRO-ACOUSTICS: PROBLEM STATEMENT AND METHODS FOR SIMULATION-BASED DESIGN SOLUTION", Proc. 8th AIAA/CEAS Aeroacoustics Conference and Exhibit, 2002.

4. VA One 2011, The ESI Group. http://www.esi-group.com

5. Cook, R. et al "Measurement of correlation coefficients in reverberant sound fields", Journal of the Acoustical Society of America, 27(6), 1955.

6. Cockburn, J.A., Robertson, J.E. "Vibration Response of Spacecraft Shrouds to In-flight Fluctuating Pressures". Journal of Sound and Vibration, 1974, 33(4), 399-425.

7. DeJong, R., Bharj, T., and Lee, J., "Vehicle Wind Noise Analysis Using a SEA Model with Measured Source Levels," SAE Technical Paper 2001-01-1629, 2001, doi: 10.4271/2001-01-1629.

8. De Jong, R., "Wind Noise Simulation Using CFD and SEA Models" Proc. ICA 2004

9. Kralicek, J. et al "Windnoise: coupling wind tunnel test data or CFD simulations to full vehicle vibro-acoustic models", Proc. DAGA 2011.

10. Peng, G., "SEA Modeling of Vehicle Wind Noise and Load Case Representation," SAE Technical Paper 2007-01-2304, 2007, doi:10.4271/2007-01-2304.

11. PAM-Flow, The ESI Group. http://www.esi-group.com

CONTACT INFORMATION

Phil Shorter
pjs@esi-group-na.com

ISSN 0148-7191

SAE Customer Service:
Tel: 877-606-7323 (inside USA and Canada)
Tel: 724-776-4970 (outside USA)
Fax: 724-776-0790
Email: CustomerService@sae.org
SAE Web Address: http://www.sae.org
Printed in USA